Transition from wakefield generation to soliton formation

Amol R. Holkundkar[1,*] and Gert Brodin[2,†]
[1]*Department of Physics, Birla Institute of Technology and Science - Pilani, Rajasthan 333031, India*
[2]*Department of Physics, Umeå University, SE-90187 Umeå, Sweden*

(Received 20 December 2017; published 16 April 2018)

It is well known that when a short laser pulse propagates in an underdense plasma, it induces longitudinal plasma oscillations at the plasma frequency after the pulse, typically referred to as the *wakefield*. However, for plasma densities approaching the critical density, wakefield generation is suppressed, and instead the EM-pulse (electromagnetic pulse) undergoes nonlinear self-modulation. In this article we have studied the transition from the wakefield generation to formation of quasi-solitons as the plasma density is increased. For this purpose we have applied a one-dimensional relativistic cold fluid model, which has also been compared with particle-in-cell simulations. A key result is that the energy loss of the EM-pulse due to wakefield generation has its maximum for a plasma density of the order 10% of the critical density, but that wakefield generation is sharply suppressed when the density is increased further.

DOI: 10.1103/PhysRevE.97.043204

I. INTRODUCTION

Wakefield generation is of fundamental interest in plasmas, both from a basic science point of view and when it comes to applications. Of particular interest is the laser wakefield acceleration scheme, which has shown tremendous progress since the pioneering work by Tajima and Dawson [1]. There are many recent experimental works directed towards electron wakefield acceleration, see, e.g., Refs. [2–4], where the particle energies in some set-ups reach the GeV regime. Three classic papers on wakefield acceleration played an important role for showing the feasibility of the plasma based accelerator concept [5–7]. Moreover, a number of different approaches for electron acceleration have been proposed and demonstrated experimentally by different research groups around the globe, e.g., bubble regime [8,9], beat wave acceleration [10,11], self-modulated laser wakefield acceleration [12], and many more. Furthermore, the effects of external magnetic fields [13], effects of modifying the laser chirp [14], and effects of varying the plasma density profile [15] on wakefield generation, have drawn considerable research interest and continue to do so.

When the electromagnetic pulses are long (as compared to the skin depth), wakefield generation is suppressed, and instead other nonlinear phenomena becomes more pronounced. Typically in a non-magnetized plasma the nonlinearity is of a focusing type, which can allow for envelope bright solitons [16]. Soliton formations have different features depending on the dimensionality, and lot of interest has been devoted to the two-dimensional (2D) [17] and three-dimensional (3D) phenomena [18]. However, when the pulses are pancake shaped, the physical scenario can be described by a one-dimensional (1D) model [19] to a good approximation. The formation and the properties of the solitonic structure in laser-plasma interaction have been widely discussed in the past [20–29]. In particular Refs. [20,23–29] have studied propagation of 1D electromagnetic pulses (EM-pulses) in an underdense plasma, focusing on phenomena such as soliton formation, and in some cases wakefield generation. While the basic equations are similar to the ones used in our paper, they have used assumptions involving a weak time-dependence (or no time-dependence in some cases) in a co-moving frame, which is relevant in many cases (e.g., for underdense plasmas; long EM-pulses and/or weak nonlinearities) but do not apply in general our case with a (sometimes) high plasma density, close to the critical density, and a very short EM-pulse of relativistic amplitude. Reference [21] has used 1D particle-in-cell (PIC) simulations, studying soliton formation in underdense plasmas, whereas Ref. [22] has studied a similar problem by solving the relativistic Vlasov equation numerically.

In the present paper we will study the competing mechanisms of linear dispersion, soliton formation, and wakefield generation, and their dependence on wave amplitude and plasma density. For this purpose we apply a 1D relativistic cold fluid model, avoiding some of the common approximations relevant for underdense plasmas. One of the main results in the present paper is that the peak in wakefield energy density occurs for densities around $n \approx 0.1 n_c$, where n is the plasma density and n_c is the critical density, but this is followed by a very sharp decrease in the wakefield energy for densities $n \gtrsim 0.2 n_c$. Furthermore, the effect of varying the laser amplitude is studied. The results from the cold relativistic fluid model are compared with particle-in-cell (PIC) simulations, and the agreement is found to be excellent.

The organization of our paper is as follows. In Sec. II the governing equations for 1D wave propagation are derived (based on a cold relativistic fluid model). Next in Sec. III the basic equations are solved numerically, and our main results are presented. In Sec. IV we make a comparison with a simplified theory and with 1D PIC simulations. Finally in Sec. V we make a summary and present the final conclusions.

*amol.holkundkar@pilani.bits-pilani.ac.in
†gert.brodin@physics.umu.se

II. THE COLD RELATIVISTIC FLUID MODEL

The main purpose of the present article is to study the propagation of a 1D electromagnetic pulse based on the cold relativistic fluid equations for electrons. Apart from treating the ions as immobile, no further approximations are made, and the equations will be solved numerically. The numerical results will be described in the next section. We assume all fields to depend on (z,t) and use the Coulomb gauge, i.e., the parallel (to z) electric field is $E_z = -\partial\phi/\partial z$ and the perpendicular electric field is given by $\mathbf{E}_\perp = -\partial\mathbf{A}/\partial t$. As has been demonstrated by, e.g., Refs. [20,25,27], the cold relativistic electron 1D equation can under these circumstances be reduced to the following form:

$$\frac{\partial^2\phi}{\partial z^2} = \frac{e(n_e - n_0)}{\varepsilon_0}, \tag{1}$$

$$\frac{\partial n_e}{\partial t} + \frac{\partial}{\partial z}(n_e v_z) = 0, \tag{2}$$

$$\frac{d}{dt}(\gamma m_e v_z) = e\frac{\partial\phi}{\partial z} - \frac{e^2}{2\gamma m_e}\frac{\partial A^2}{\partial z}, \tag{3}$$

and

$$\frac{\partial^2\mathbf{A}}{\partial z^2} - \frac{1}{c^2}\frac{\partial^2\mathbf{A}}{\partial t^2} = \frac{\mu_0 e n_e \mathbf{A}}{\gamma m_e}, \tag{4}$$

where e and m_e is the electron charge, n_e is the electron number density, n_0 represents the (constant) neutralizing background, v_z is the parallel component of the velocity $d/dt \equiv \partial/\partial t + v_z\partial/\partial z$, the relativistic γ factor can be written as

$$\gamma = \sqrt{\frac{1+a^2}{1 - v_z^2/c^2}} \tag{5}$$

and we have introduced the normalized vector potential $a^2 = (e\mathbf{A}/m_e c)^2$. While Eqs. (1)–(5) constitute a closed set, they are nontrivial to use as they stand, as the longitudinal momentum equation (3) contains a temporal derivative both on v_z and on γ (and thereby indirectly on a^2). This has typically been dealt with by introducing various approximations (usually involving a slow evolution of the electromagnetic fields in a co-moving frame). However, here we do not limit ourselves to plasmas that are undercritical by a large margin and hence we have no small parameter that justifies ansatzes for the vector or scalar potential involving slowly varying fields. Instead we rewrite Eq. (3) as

$$\frac{dv_z}{dt} = \frac{e}{\gamma m_e}\frac{\partial\phi}{\partial z} - \frac{e^2}{2\gamma^2 m_e^2}\frac{\partial A^2}{\partial z} - \frac{v_z}{\gamma}\frac{d\gamma}{dt}. \tag{6}$$

Noting that the rate of change of the energy is given by $d\mathcal{E}/dt = -e\mathbf{v}\cdot\mathbf{E}$, where $\mathcal{E} = \gamma m_e c^2$, we find

$$\frac{d\gamma}{dt} = \frac{e}{m_e c^2}\left(v_z\frac{\partial\phi}{\partial z} + \frac{e}{2\gamma m_e}\frac{\partial A^2}{\partial t}\right). \tag{7}$$

Combining Eqs. (6) and (7) the evolution equation for v_z becomes

$$\frac{dv_z}{dt} = \frac{e}{\gamma m_e}\left(1 - \frac{v_z^2}{c^2}\right)\frac{\partial\phi}{\partial z} - \frac{e^2}{2\gamma^2 m_e^2}\left(\frac{\partial A^2}{\partial z} + \frac{v_z}{c^2}\frac{\partial A^2}{\partial t}\right). \tag{8}$$

In principle Eq. (8) together with Eqs. (1), (2), (4), and (5) already form a closed set. However, for convenience we chose to work with evolution equations for all our dynamical variables, and hence we let the z-component of Ampere's law

$$\frac{1}{c^2}\frac{\partial^2\phi}{\partial t\partial z} = -\mu_0 e n_e v_z \tag{9}$$

replace Poisson's equation.

Next we introduce the normalizations $\mathbf{a} = e\mathbf{A}/m_e c$ and $\varphi = e\phi/m_e c^2$ for the vector and scalar potential, respectively. Furthermore, time and space are normalized against the laser frequency and wave number ($\omega t \to t$ and $kx \to x$), respectively. The parallel velocity is normalized against the speed of light, $\beta = v_z/c$, and finally the electron density is normalized against the critical density $n_c = \varepsilon_0\omega^2 m_e/e^2$ (from now on n_e represents n_e/n_c). By using these normalizations our basic equations are written as

$$\frac{\partial^2\mathbf{a}}{\partial z^2} - \frac{\partial^2\mathbf{a}}{\partial t^2} = n_e\frac{\mathbf{a}}{\gamma}, \tag{10}$$

$$\frac{d\beta}{dt} = \frac{(1-\beta^2)}{\gamma}\frac{\partial\varphi}{\partial z} - \frac{1}{2\gamma^2}\left(\frac{\partial\mathbf{a}^2}{\partial z} + \beta\frac{\partial\mathbf{a}^2}{\partial t}\right), \tag{11}$$

$$\frac{\partial n_e}{\partial t} + \frac{\partial}{\partial z}(n_e\beta) = 0, \tag{12}$$

$$\gamma = \sqrt{\frac{1+a^2}{1-\beta^2}}, \tag{13}$$

$$\frac{\partial^2\varphi}{\partial t\partial z} = -n_e\beta. \tag{14}$$

Equations (10)–(14) constitute the basis for the result presented below.

III. RESULTS

We have solved Eqs. (10)–(14) numerically in the same sequence for the case of a localized EM-pulse entering the simulation box from the left side. The simulation box has been varied in size from 275–750λ in the various simulations, with a constant unperturbed plasma density n_0 throughout the box length. The linearly polarized Gaussian laser pulse of wavelength 800 nm has a full width at half-maximum (FWHM) duration of 5 cycles ($\tau_{\mathrm{FWHM}} = 5\times 2\pi$). The normalized amplitude a_0 is varied in the different simulations, and the pulse is launched from the left boundary of the simulation box. The boundary conditions on the left boundary read as

$$\mathbf{a}(0,t) = a_0\exp\left(-\frac{4\log(2)t^2}{\tau_{\mathrm{FWHM}}^2}\right)\cos(t)\ \hat{\mathbf{x}}, \tag{15}$$

$$n_e(0,t) = n_0, \tag{16}$$

$$\beta(0,t) = \varphi'(0,t) = 0 \quad (\varphi' \equiv \partial\varphi/\partial z). \tag{17}$$

In the following we present the results by solving the fluid equations. The results are categorized in different subsections for pedagogical reasons.

A. The transition from dispersive to non-dispersive pulses

In Fig. 1, we have presented the wakefield generation for a low amplitude laser pulse. The interaction of 5 cycle Gaussian laser pulses with peak amplitude $a_0 = 0.01$ with an

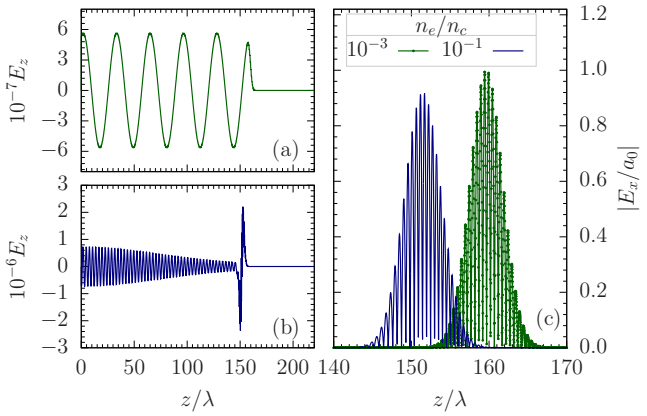

FIG. 1. The spatial profiles of longitudinal field are plotted at $t = 159$ for the case when a 5 cycle laser pulse with $a_0 = 0.01$ interacts with a plasma having density $0.001n_c$ (a) and $0.1n_c$ (b). The corresponding spatial profiles of the transverse field (EM driver) are also presented in (c) [profile on right (left) is for $0.001n_c$ ($0.1n_c$)].

unperturbed plasma with a density of $0.001n_c$ and $0.1n_c$ is considered, and the spatial profiles of longitudinal [Figs. 1(a),1(b)] and transverse [Fig. 1(c)] fields as evaluated at $t = 159$ are shown.

For the lower density we see that the longitudinal field has a pure wakefield nature, i.e., harmonic oscillations are induced after the peak of the EM-pulse. Moreover, since dispersive effects are very small for such a low density, the wakefield generation continues more or less unchanged for a long time. By contrast, for a density of $0.1n_c$ the longitudinal fields still have a pronounced wakefield, but there is also a strong peak where the EM-pulse is localized. Furthermore, for the low amplitude $a_0 = 0.01$ the wakefield amplitude is largest directly after the pulse entrance, and then the wakefield amplitude is gradually decreasing. The reason for the diminishing wakefield amplitude is the EM-wave dispersion, which becomes significant for densities of order $0.1n_c$ and higher. This can be verified by studying Fig. 2. In Fig. 2(d) we see the EM-wave profile for $a_0 = 0.01$ at $t = 109, 409, 749$ (note the pulse broadening). As a result of the pulse broadening, the wakefield generation is decreasing, as can be seen from the longitudinal field displayed in Fig. 2(a).

When the amplitude is increased, the nonlinearity begins to counteract dispersion, which means that wakefield generation can be sustained. We compare the EM-wave profile for $a_0 = 0.01$, $a_0 = 0.1$, and $a_0 = 0.3$ at $t = 109, 409, 749$ in the right panel of Fig. 2. While there is some tendency to decreased dispersion for $a_0 = 0.1$, the main suppression of dispersion occurs when increasing the amplitude up to $a_0 = 0.3$. The result for the longitudinal fields is quite dramatic, as seen when comparing the corresponding profiles in the left panel of Fig. 2. Note that wakefield generation is completely suppressed due to pulse broadening both for $a_0 = 0.01$ and $a_0 = 0.1$, although the suppression takes somewhat longer in the latter case. By contrast, the prevention of pulse broadening for $a_0 = 0.3$ means that wakefield generation can be sustained for a long time. Naturally, the energy loss due to wakefield generation will eventually decrease the EM wave amplitude, such that the degree of nonlinearity is reduced and dispersion sets in, but that will take much longer time.

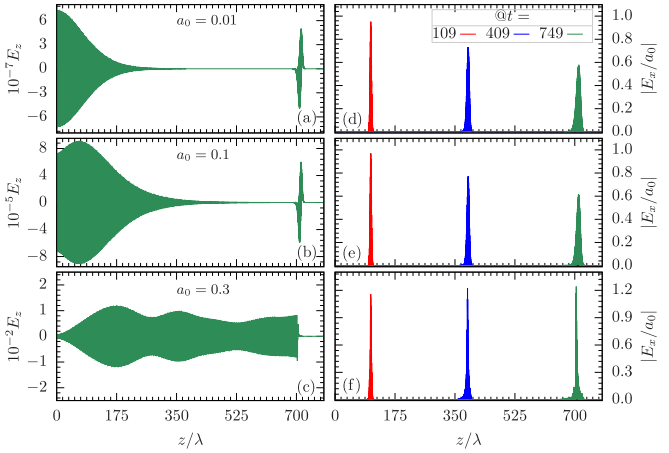

FIG. 2. The spatial profiles of the longitudinal field (left panel) are plotted at $t = 749$ for the cases when a 5 cycle laser pulse with $a_0 = 0.01$ (a), 0.1 (b), and 0.3 (c) interacts with a plasma having density $0.1n_c$. The spatial profiles of the transverse field with $a_0 = 0.01$ (d), 0.1 (e), and 0.3 (f) are also presented in right panel for $t = 109$ (left), 409 (center), and 749 (right).

B. The transition from wakefield generation to soliton formation

In Fig. 3, the spatial profile of longitudinal field $E_z = -\varphi'$ for different plasma densities calculated at $t = 263$ (∼42 cycles) is presented by solving Eqs. (10)–(14) numerically for $a_0 = 0.3$. Varying the density from $n = 0.001n_c$ up to $n = 0.6n_c$ we note that the longitudinal field is a pronounced wakefield for the lower densities, but gradually turns into a driven field that is localized to the same region as the EM field that drives the perturbation. As we increase the initial plasma density, the wakefield amplitude decreases and eventually a soliton like structure propagates in the plasma.

The time evolution of the transverse pulse profile for $a_0 = 0.3$ and $n_e = 0.6n_c$ is presented in Fig. 4(b), along with the corresponding longitudinal field Fig. 4(a). As we can see, the nonlinearity prevents dispersion for most of the energy

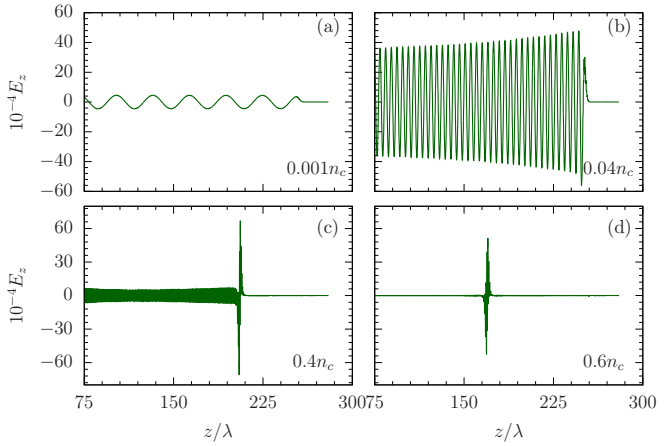

FIG. 3. Fluid simulation: The wakefield for different plasma densities $0.001\,n_c$ (a), $0.04n_c$ (b), $0.4n_c$ (c), and $0.6n_c$ (d) are presented as calculated at $t = 263$. The laser parameters are $a_0 = 0.3$, 5 cycle (FWHM) Gaussian linearly polarized laser pulse, incident on the plasma slab of 275λ.

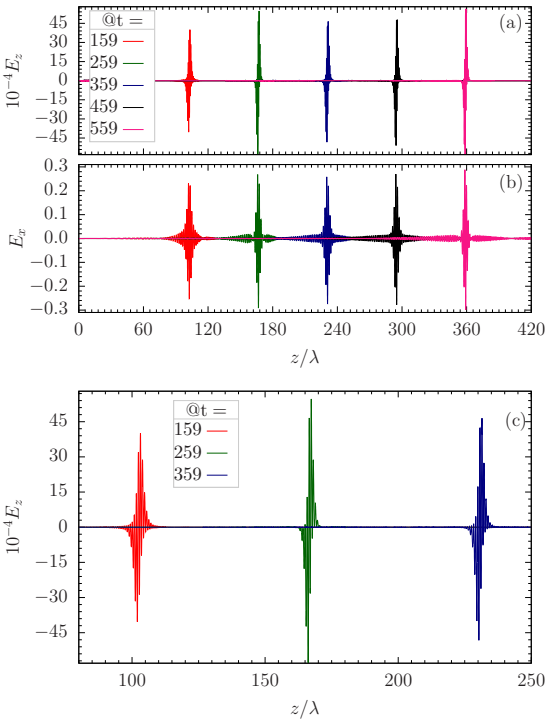

FIG. 4. Spatiotemporal evolution of electrostatic (a), electromagnetic (b) fields with 5 cycle laser with amplitude $a_0 = 0.3$ and $n_e = 0.6n_c$. Enlarged version of the solitonic structures is also presented separately (c). In all panels, field profiles are illustrated from left to right with ascending temporal order.

contained in the pulse, and the central part of the pulse tends to shorten over time. As a result the longitudinal field driven by the transverse part tend to increase somewhat over time. However, we also see that the high- and low-frequency parts of the pulse spectrum tend to irradiate forwards and backwards, respectively. Apart from this irradiation, which represents a relatively minor energy loss of the central part of the EM-pulse, the pulse profile approaches a more or less fixed shape. We will refer to these structures as "*quasi-solitons*". We cannot exclude that true soliton-formation eventually occurs, but for the rather long time-span that we follow, we see a process where parts of the frequency spectrum are irradiated backwards and forwards. To give a more clear view of the longitudinal pulse profile, we present a zoom of the longitudinal fields for three different times in Fig. 4(c).

C. Energy loss as a function of density

For a density much less than the critical density, wakefield generation is the dominant process, as seen, e.g., in Fig. 3(a). However, due to the limited number of particles, the longitudinal field cannot store a very high energy density, and thus the energy loss for the transverse degrees of freedom (=the electromagnetic pulse) is limited. For a high plasma density (i.e., not much smaller than the critical density), wakefield generation is almost completely suppressed, and there is negligible energy loss to the longitudinal degrees of freedom, see Fig. 3(d). These simple observations imply that there is an intermediate plasma density where the energy loss

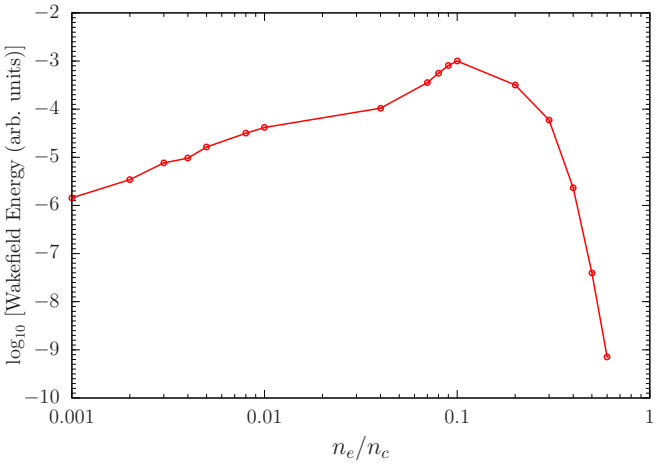

FIG. 5. The wakefield energy is calculated as $\int_{z_0}^{z_1} |E_z|^2 dz$. Here, z_0 and z_1 are 20λ and 10λ behind the peak of the laser at $t = 263$ for different plasma densities.

due to wakefield generation has its maximum. The purpose of this subsection is to determine this characteristic value.

As we have seen in [Figs. 2(a), 2(b)], for the higher plasma densities wakefield generation will be suppressed due to dispersion, unless the amplitude is strong enough to keep the pulse short enough, as in Fig. 2(c). To avoid dispersive suppression we will consider pulse amplitudes firmly in the nonlinear (=non-dispersive) regime and pick $a_0 = 0.3$. We are interested in the dependence of the wakefield energy as a function of density (rather than the absolute value), and therefore we have used the integral $\int_{z_0}^{z_1} |E_z|^2 dz$ as a measure. Here, z_0 and z_1 are 20λ and 10λ behind the peak of the laser computed at $t = 263$ for a given plasma density. Note that the wakefield will divide its energy equally between kinetic energy and electrostatic field energy, unless we are in an extremely nonlinear regime. The generated wakefield energy as a function of the plasma density is presented in Fig. 5. Initially the wakefield energy increases with density, as expected from standard theory of wakefield generation. The maximum peak of the wakefield energy is reached for a density of the order $0.1n_c$. However, if we further increase the plasmas density beyond approximately $n_e \sim 0.2n_c$, there is rapid drop in the wakefield energy. The drop in wakefield energy coincides with the formation of solitary pulses which we label quasi-solitons, as discussed in the previous subsection.

IV. COMPARISON WITH THEORY AND PIC-SIMULATIONS

A first theoretical estimate of the propagation velocity for the EM-pulses can be found by computing the group velocity including a nonlinear correction for the relativistic factor induced by the EM field. In linearized theory the group velocity can be calculated as

$$v_g = c\sqrt{1 - \omega_p^2/\omega^2} = c\sqrt{\varepsilon}. \tag{18}$$

To get a first estimate of the amplitude dependence, we can replace the unperturbed plasma frequency with the value corrected by the γ factor due the transverse motion in the

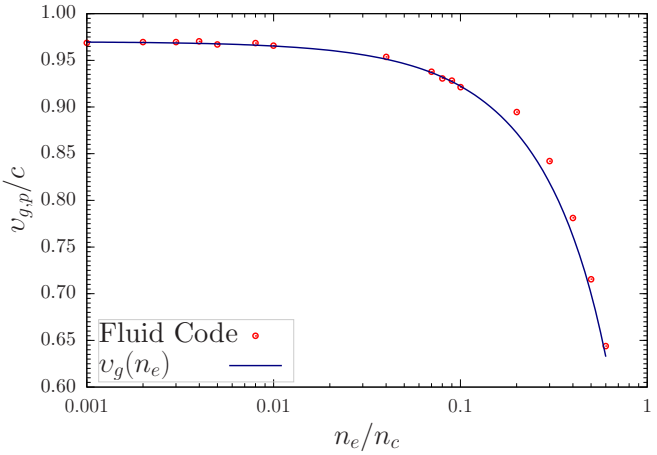

FIG. 6. A comparison of the group velocity v_g, the line fitted by Eq. (19), and the propagation velocity v_p, the dots computed from the position of the central peak of the EM field, as a function of plasma density. Here, the case of a 5 cycle EM pulse with $a_0 = 0.3$ is considered.

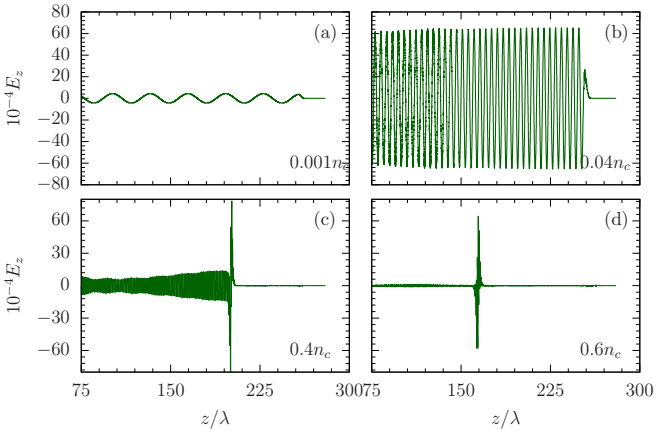

FIG. 7. PIC simulation: The wakefields for different plasma densities $0.001n_c$ (a), $0.04n_c$ (b), $0.4n_c$ (c), and $0.6n_c$ (d) are presented as calculated at $t = 265$. The laser parameters are $a_0 = 0.3$, 5 cycle (FWHM) Gaussian linearly polarized laser pulse, incident on the plasma slab of 275λ.

EM-field. This suggests that the expression from linearized theory can be substituted as $ne^2/\varepsilon_0 m_e \to ne^2/\varepsilon_0 \gamma m_e$, where we let $\gamma = \sqrt{1 + a_0^2}$, where we use the normalized peak vector potential. Using the peak potential overestimates the average γ factor, but ignoring the contribution from the longitudinal motion underestimates it. Hence this may serve as a rough estimate for the propagation velocity. The expression which we will compare with the results from the numerical code is now given by

$$v_g = c\sqrt{1 - \frac{n_e}{n_c\sqrt{1 + a_0^2}}}. \tag{19}$$

In spite of the rather crude estimates involved, we see that the propagation velocity computed by the fluid code (simply based on the position of the central peak of the EM-field) agrees very well with the expression (19), as we can see in Fig. 6. Here, the propagation velocity is plotted as a function of density for the case of $a_0 = 0.3$.

Next we turn to a comparison of the fluid code with PIC simulations. The 1D particle-in-cell simulation (LPIC++) [30] is carried out to study the effect of plasma densities on the wakefield generation. This is freely available 1D-3V open-source PIC simulation package, developed mainly to study the laser-plasma interaction. For the results presented here the EM field amplitude of the driver is considered to be $a_0 = 0.3$ (in dimensionless unit $a_0 = eE/m_e\omega c$, with ω being the frequency), space and time are taken in units of laser wavelength (λ) and one laser cycle $\tau = \lambda/c$, respectively, mass and charge are normalized with electron mass and charge, respectively. We have used 50 cells per laser wavelength with each cell having 50 electron and ion macroparticles. The spatial grid size and temporal time step for the simulation is considered to be 0.02λ and 0.02τ, respectively. Though in PIC simulation we have considered the ion mass $m_i \sim 1836m_e$, but on the timescale of interests ions can be treated as immobile, consistent with the fluid model. The 800 nm laser with FWHM duration of 5τ and an initially Gaussian shape propagates through the plasma along the z-direction with electric field along x-direction. The plasma of length 275 λ is considered having uniform density n_0 (in units of n_c). The laser parameters used ($a_0 = 0.3$ with FWHM of 5τ) would translate to the ∼10 fs (intensity FWHM) laser pulse having peak intensity $\sim 2\times 10^{17}$ W/cm^2.

In Fig. 7, the spatial profile of longitudinal field E_z for different plasma densities calculated at $t = 265$ is presented. It can be seen that for low plasma densities we have wakefield generation behind the laser pulse for low density plasmas ($0.001 \leqslant n_e \leqslant 0.04n_c$). However, as the plasma density increases the wakefield amplitude decreases and eventually we have only a soliton-like structure propagating in the plasma for say $n_e = 0.6n_c$. These results are in good agreement with the fluid results, as can be seen by comparing with the corresponding results from the fluid code shown in Fig. 3.

V. SUMMARY AND DISCUSSION

Starting from equations presented in previous works (e.g., Refs. [20,25,27]), we have derived a cold, fully relativistic 1D model, that we have solved numerically. The purpose has been to study the competition between linear dispersion, nonlinear self-modulation, and wakefield generation for a localized electromagnetic pulse propagating in a homogeneous non-magnetized plasma. First we have deduced that wakefield generation for initially short pulses is suppressed by linear dispersion after a relatively short time, if the plasma density is modest or high (i.e., of the order $0.1n_c$ or higher) unless the normalized amplitude is of the order $a_0 \simeq 0.3$. In case we are firmly in the nonlinear regime, the nonlinear self-modulation keep the pulse short enough to sustain wakefield generation for a long time—until depletion due to the wakefield generation becomes significant. When the plasma density is increased further, wakefield generation is replaced by a formation of quasi-solitons. The central part of the pulse propagates with very little changes of the pulse shape, but a small irradiation backward and forward of the low-frequency

and high-frequency part of the spectrum still occurs. A key part of the present study is the scaling with the plasma density of the energy loss of the EM-pulse due to wakefield generation. For pulses in the nonlinear regime (not suffering dispersive broadening), we find that the energy loss has a maximum when the plasma density is of the order $n \simeq 0.1 n_c$. When the plasma density is increased beyond $n \simeq 0.2 n_c$ there is a rapid decrease of the wakefield energy with the plasma density, signaling the onset of (quasi)soliton formation. The results produced by the fluid code have been checked against 1D PIC simulations, and the agreement has been found to be excellent.

Many of the conclusions in the present paper have a rather general nature, as the competition between dispersion, wakefield generation and self-modulation may take place in a magnetized plasma, and also for different types of wave modes. Qualitatively many of the features of the present study can be assumed to hold in a more general context, as long as the nonlinear self-modulation is of focusing type. In particular wakefield generation is more prominent for short wave packets (which may be of electromagnetic or electrostatic nature), and are likely to be suppressed by dispersive broadening, unless the nonlinear self-modulation prevents this from happening. Moreover, the energy loss due to wakefield generation is likely to be suppressed for low and high plasma densities (for a given wave frequency). Thus the existence of a plasma density that optimizes wakefield generation is likely a generic feature. To what extent the conclusions reported here hold also for electromagnetic waves propagating in a magnetized plasma remains an issue for further research.

ACKNOWLEDGMENTS

A.H. acknowledges the Department of Physics, Umeå University, Sweden for the local hospitality and the travel support. A.H. also acknowledges the Max Planck Institute for the Physics of Complex Systems, Dresden, Germany for the financial support. G.B. would like to acknowledge financial support by the Swedish Research Council, Grant No. 2016-03806.

[1] T. Tajima and J. M. Dawson, Phys. Rev. Lett. **43**, 267 (1979).
[2] S. Kneip, S. R. Nagel, S. F. Martins, S. P. D. Mangles, C. Bellei, O. Chekhlov, R. J. Clarke, N. Delerue, E. J. Divall, G. Doucas, K. Ertel, F. Fiuza, R. Fonseca, P. Foster, S. J. Hawkes, C. J. Hooker, K. Krushelnick, W. B. Mori, C. A. J. Palmer, K. Ta Phuoc, P. P. Rajeev, J. Schreiber, M. J. V. Streeter, D. Urner, J. Vieira, L. O. Silva, and Z. Najmudin, Phys. Rev. Lett. **103**, 035002 (2009).
[3] H. T. Kim, K. H. Pae, H. J. Cha, I. J. Kim, T. J. Yu, J. H. Sung, S. K. Lee, T. M. Jeong, and J. Lee, Phys. Rev. Lett. **111**, 165002 (2013).
[4] W. P. Leemans, A. J. Gonsalves, H.-S. Mao, K. Nakamura, C. Benedetti, C. B. Schroeder, C. Tóth, J. Daniels, D. E. Mittelberger, S. S. Bulanov, J.-L. Vay, C. G. R. Geddes, and E. Esarey, Phys. Rev. Lett. **113**, 245002 (2014).
[5] S. P. D. Mangles, C. D. Murphy, Z. Najmudin, A. G. R. Thomas, J. L. Collier, A. E. Dangor, E. J. Divall, P. S. Foster, J. G. Gallacher, C. J. Hooker, D. A. Jaroszynski, A. J. Langley, W. B. Mori, P. A. Norreys, F. S. Tsung, R. Viskup, B. R. Walton, and K. Krushelnick, Nature **431**, 535 (2004).
[6] J. Faure, Y. Glinec, A. Pukhov, S. Kiselev, S. Gordienko, E. Lefebvre, J.-P. Rousseau, F. Burgy, and V. Malka, Nature **431**, 541 (2004).
[7] C. G. R. Geddes, C. Toth, J. van Tilborg, E. Esarey, C. B. Schroeder, D. Bruhwiler, C. Nieter, J. Cary, and W. P. Leemans, Nature **431**, 538 (2004).
[8] B. Shen, Y. Li, M. Y. Yu, and J. Cary, Phys. Rev. E **76**, 055402 (2007).
[9] B. Hidding, T. Königstein, J. Osterholz, S. Karsch, O. Willi, and G. Pretzler, Phys. Rev. Lett. **104**, 195002 (2010).
[10] C. V. Filip, R. Narang, S. Ya. Tochitsky, C. E. Clayton, P. Musumeci, R. B. Yoder, K. A. Marsh, J. B. Rosenzweig, C. Pellegrini, and C. Joshi, Phys. Rev. E **69**, 026404 (2004).
[11] R. M. G. M. Trines, Phys. Rev. E **79**, 056406 (2009).
[12] N. Hafz, M. S. Hur, G. H. Kim, C. Kim, I. S. Ko, and H. Suk, Phys. Rev. E **73**, 016405 (2006).
[13] A. Holkundkar, G. Brodin, and M. Marklund, Phys. Rev. E **84**, 036409 (2011).
[14] V. B. Pathak, J. Vieira, R. A. Fonseca, and L. O. Silva, New J. Phys. **14**, 023057 (2012).
[15] A. Pukhov and I. Kostyukov, Phys. Rev. E **77**, 025401 (2008).
[16] M. Y. Yu, P. K. Shukla, and N. L. Tsintsadze, Phys. Fluids **25**, 1049 (1982).
[17] N. M. Naumova, S. V. Bulanov, T. Z. Esirkepov, D. Farina, K. Nishihara, F. Pegoraro, H. Ruhl, and A. S. Sakharov, Phys. Rev. Lett. **87**, 185004 (2001).
[18] T. Esirkepov, K. Nishihara, S. V. Bulanov, and F. Pegoraro, Phys. Rev. Lett. **89**, 275002 (2002).
[19] D. Jovanović, R. Fedele, M. Belić, and S. D. Nicola, Phys. Plasmas **22**, 043110 (2015).
[20] P. K. Kaw, A. Sen, and T. Katsouleas, Phys. Rev. Lett. **68**, 3172 (1992).
[21] S. V. Bulanov, T. Z. Esirkepov, N. M. Naumova, F. Pegoraro, and V. A. Vshivkov, Phys. Rev. Lett. **82**, 3440 (1999).
[22] P. K. Shukla and B. Eliasson, Phys. Rev. Lett. **94**, 065002 (2005).
[23] G. Sánchez-Arriaga, E. Siminos, V. Saxena, and I. Kourakis, Phys. Rev. E **91**, 033102 (2015).
[24] E. Siminos, G. Sánchez-Arriaga, V. Saxena, and I. Kourakis, Phys. Rev. E **90**, 063104 (2014).
[25] V. Saxena, I. Kourakis, G. Sanchez-Arriaga, and E. Siminos, Phys. Lett. A **377**, 473 (2013).
[26] V. Saxena and I. Kourakis, Europhys. Lett. **100**, 15002 (2012).
[27] V. Saxena, A. Sen, and P. Kaw, Phys. Rev. E **80**, 016406 (2009).
[28] G. Sánchez-Arriaga, E. Siminos, and E. Lefebvre, Plasma Phys. Controlled Fusion **53**, 045011 (2011).
[29] L. Hadžievski, M. S. Jovanović, M. M. Škorić, and K. Mima, Phys. Plasmas **9**, 2569 (2002).
[30] R. Lichters, R. E. W. Pfund, and J. Meyer-Ter-Vehn, Max-Planck Institute for Quantum Optics, Report No: MPQ-225 (1997).